Published in final edited form as:
Nat Chem Biol. 2011 March ; 7(3): 174–181. doi:10.1038/nchembio.520.

Hijacking a biosynthetic pathway yields a glycosyltransferase inhibitor within cells

Tracey M. Gloster[1], **Wesley F. Zandberg**[1], **Julia E. Heinonen**[1], **David L. Shen**[2], **Lehua Deng**[1], and **David J. Vocadlo**[1,2]

[1] Department of Chemistry, Simon Fraser University, 8888 University Drive, Burnaby, V5A 1S6, Canada.

[2] Department of Molecular Biology and Biochemistry, Simon Fraser University, 8888 University Drive, Burnaby, V5A 1S6, Canada.

Abstract

Glycosyltransferases (GTs) are ubiquitous enzymes that catalyze the assembly of glycoconjugates found throughout all kingdoms of nature. A longstanding problem is the rational design of probes that can be used to manipulate GT activity in cells and tissues. Here we describe the rational design and synthesis of a nucleotide sugar analogue that inhibits, with high potency both *in vitro* and in cells, the human GT responsible for the reversible post-translational modification of nucleocytoplasmic proteins with *O*-linked *N*-acetylglucosamine residues (*O*-GlcNAc). We show the enzymes of the hexosamine biosynthetic pathway can transform, both *in vitro* and in cells, a synthetic carbohydrate precursor into the nucleotide sugar analogue. Treatment of cells with the precursor decreases *O*-GlcNAc in a targeted manner with a single digit micromolar EC_{50}. This approach to inhibition of GTs should be applicable to other members of this increasingly interesting superfamily of enzymes and enable their manipulation in a biological setting.

The formation of glycoconjugates is nearly always mediated by GT-catalyzed transfer of a sugar residue from an anionic nucleotide sugar donor to various acceptors molecules, which may be proteins, lipids, saccharides, or metabolites. Mammals have over 200 GTs that give rise to diverse glycoconjugates and these structures are emerging as regulators of quality control, cellular structure, signaling, gene transcription, and intercellular communication[1] as well as potential therapeutic targets[2]-[4]. A longstanding problem, which has somewhat hindered progress in glycobiology, is the rational design of chemical tools that can be used to manipulate GT activity in cells and tissues; such reagents would be powerful probes that would aid in defining the precise biological functions of GTs. For this reason, considerable effort has been directed into the design of GT inhibitors. Most rationally designed inhibitors emulate nucleotide phosphate sugars and incorporate anionic groups to capture binding energy associated with the phosphate bridge of nucleotide phosphosugar substrates. While many of these inhibitors have been found to be potent in *in vitro* assays, they typically do not permeate into cells owing to their highly polar and charged nature. Accordingly, there is a need for new strategies to inhibit GTs in cells and tissues.

Corresponding author: David J. Vocadlo, Tel: 001 778 782 3530, Fax: 001 778 782 3765..

Author contributions

T.M.G. and D.J.V. designed experiments. T.E.G., W.F.Z., J.E.H., D.L.S., and L.D. performed experiments. T.M.G., W.F.Z., D.L.S., and D.J.V. analyzed results. T.M.G. and D.J.V wrote the manuscript with input from all authors.

Competing financial interests

Provisional patent applications covering this work have been filed.

Europe PMC Funders Author Manuscripts

One particular form of post-translational glycosylation that is of considerable interest is the modification of intracellular proteins with 2-acetamido-2-deoxy-D-glucopyranose (GlcNAc, **1**, Figure 1a) β-glycosidically linked to serine or threonine residues of proteins (*O*-GlcNAc)[5]. *O*-GlcNAc is a nuclear and cytoplasmic modification ubiquitously found in all multicellular eukaryotes. Several hundred proteins, involved in a wide range of cellular functions, are modified with *O*-GlcNAc[5]. *O*-GlcNAc is generally substoichiometric on proteins[5] and can be installed and removed several times during the lifetime of a given protein[6]. Its cycling is regulated by two enzymes; a GT (uridine diphospho-*N*-acetylglucosamine:polypeptide β-*N*-acetylglucosaminyltransferase; OGT)[5], which transfers *O*-GlcNAc onto proteins, and a glycoside hydrolase (*O*-GlcNAcase; OGA)[5] that removes *O*-GlcNAc. *O*-GlcNAc has been proposed to mediate critical cellular processes in nutrient signaling[7], regulation of gene transcription[8], cellular stress response[9] and cell division[10].

Given the current interest in the role of *O*-GlcNAc, and the potential therapeutic benefits that might be associated with manipulating *O*-GlcNAc levels[11-15], there is a need for useful chemical tools to probe this modification. Current chemical approaches to reduce *O*-GlcNAc levels generally suffer shortcomings. 6-diazo-5-oxo-L-norleucine and L-azaserine block uridine diphospho-*N*-acetylglucosamine (UDP-GlcNAc, **2**, Figure 1a) biosynthesis but inhibit other amidotransferases including those involved in purine and pyrimidine biosynthesis and also cause DNA damage[16]. Alloxan, a uracil analogue, has been proposed to inhibit OGT, but is toxic and affects many cellular processes[17]. More recently however, OGT inhibitors discovered by library screening[18] have shown some utility in cells[11,19]. Due to the interest in the biological functions of *O*-GlcNAc and its proposed links to many diseases, we were motivated to rationally design an inhibitor that could be used effectively in cells.

The donor substrate used by OGT, UDP-GlcNAc (**2**), is biosynthesized through the action of the enzymes comprising the hexosamine biosynthetic pathway (HBP) and the GlcNAc salvage pathway (Figure 1b). Interestingly, nucleotide sugar biosynthetic pathways[20-22], including the HBP[23], have been shown to tolerate various sugar analogues, which enables the biosynthesis of unnatural glycan structures within cells[20-23]. We felt that these pathways could be exploited in a different way to generate GT inhibitors. By treating tissues with a cell permeable biosynthetic precursor we hypothesized that the HBP, as an exemplar, could be hijacked to generate within cells an OGT inhibitor having the important pyrophosphate bridge. Given that GTs use a catalytic mechanism involving a cationic transition state in which the geometry of the pyranose ring likely plays a critical role[24], we felt that 2-acetamido-2-deoxy-5-thio-D-glucopyranose (5SGlcNAc, **3**, Figure 1a), wherein the endocyclic ring oxygen of GlcNAc is replaced with a sulfur atom, would be a good candidate. Other 5-thiosugars have been explored as inhibitors of glycoside hydrolases[25] and nucleotide 5-thiosugar analogues of different sugars have been tested as substrates for GTs *in vitro*[26-28]. Interestingly, in cases where the GT-catalyzed glycosyl transfer from nucleotide 5-thiosugar donors has been assayed, the efficiency of transfer is only between 0.2 and 5% compared to the natural nucleotide sugar donor[26-28]. This less efficient transfer of 5-thiosugars may be due to the distorted conformation of the pyranose ring that is known to be adopted by these compounds relative to their oxygen counterparts[29]. Therefore, we speculated that OGT would be inhibited by uridine diphospho-5-thio-*N*-acetylglucosamine (UDP-5SGlcNAc, **4**, Figure 1a) and that, although UDP-5SGlcNAc (**4**) might be turned over, the rate of transfer would be sufficiently slow that it would essentially act as an inhibitor in cells. Here we show that 5SGlcNAc (**3**) and its per-*O*-acetylated analogue, 2-acetamido-1,3,4,6-tetra-*O*-acetyl-2-deoxy-5-thio-α-D-glucopyranose (Ac-5SGlcNAc, **5**, Figure 1a), can be salvaged by cells and processed via the HBP to generate UDP-5SGlcNAc (**4**), which acts as an inhibitor of OGT and leads to decreases in cellular *O*-GlcNAc levels.

Results

Synthesis of UDP-5SGlcNAc and in vitro evaluation

To establish feasibility of our proposed strategy we first evaluated whether 5SGlcNAc (**3**) could be transformed into UDP-5SGlcNAc (**4**) by the human enzymes of the HBP and GlcNAc salvage pathway. Chemoenzymatic synthesis of nucleotide sugars *in vitro* using bacterial enzymes is well precedented[30], however, there have been no studies reporting the biosynthesis of nucleotide 5-thiosugars using mammalian enzymes. As a first step we synthesized 5SGlcNAc (**3**) essentially as described previously but with minor modifications[31] (see Supplementary Methods and Supplementary Scheme 1). Using this material, UDP-5SGlcNAc (**4**) was prepared in a one-pot reaction containing 5SGlcNAc (**3**), ATP, UTP, and recombinant human GlcNAc kinase (GNK), GlcNAc mutase (AGM) and UDP-GlcNAc pyrophosphorylase (AGX1). Monitoring the reaction by capillary electrophoresis (CE), revealed the formation of a new nucleotide sugar (Supplementary Figure 1a). This product was purified and characterization of the purified material was consistent with its identity being UDP-5SGlcNAc (**4**, Supplementary Figures 2-4). We then assayed the ability of OGT to use UDP-5SGlcNAc (**4**) as a donor using nuclear pore protein p62 (nup62) as a substrate[32,33]. We found UDP-5SGlcNAc (**4**) is a 14-fold worse substrate ($Rate_{UDP\text{-}5SGlcNAc}$ = 0.86 pmol·min^{-1}·mg OGT^{-1}) than UDP-GlcNAc (**2**, $Rate_{UDP\text{-}GlcNAc}$ = 12.1 pmol·min^{-1}·mg OGT^{-1}). It is important to note that these values reflect the rate of processing of UDP-GlcNAc (**2**) and UDP-5SGlcNAc (**4**), and are composites of both hydrolysis and transfer to protein. Therefore this measured rate for UDP-5SGlcNAc (**4**) processing is an absolute upper limit for the OGT-catalyzed transfer of 5SGlcNAc (**3**) onto proteins. Nevertheless, it is possible that OGT transfers 5SGlcNAc (**3**) to proteins within cells, although the rate of transfer is clearly poor at best. Consequently, we felt it was important to establish whether OGA could cleave 5SGlcNAc (**3**) glycosides since, if OGA were unable to do so, levels of 5SGlcNAc-modified proteins might accumulate within cells treated with 5SGlcNAc (**3**) or Ac-5SGlcNAc (**5**). We therefore assayed *para*-methoxyphenyl 2-acetamido-2-deoxy-β-D-glucopyranoside[34] (*p*MP-GlcNAc, **6**, Figure 1a) and synthesized its sulfur containing counterpart *para*-methoxyphenyl 2-acetamido-2-deoxy-5-thio-β-D-glucopyranoside (*p*MP-5SGlcNAc, **7**, Figure 1a, see Supplementary Methods and Supplementary Scheme 2 for details of the synthesis and characterization) and evaluated the OGA-catalyzed hydrolysis of these compounds. Michaelis-Menten kinetics (Supplementary Figures 5a, b) reveal human OGA processes *p*MP-5SGlcNAc (**7**, V_{max}/E_0K_M = 8.1 μmol s^{-1} mg^{-1} M^{-1}) only 5-fold less efficiently than *p*MP-GlcNAc (**6**, V_{max}/E_0K_M = 40.7 μmol s^{-1} mg^{-1} M^{-1}), indicating that 5SGlcNAc (**3**) adventitiously transferred onto proteins within cells by OGT to form *O*-5SGlcNAc would very likely be removed more efficiently than it is installed. These enzymological studies on the processing of 5SGlcNAc-containing substrates suggest that 5SGlcNAc (**3**) would not accumulate on proteins within cells and supports the view that this general strategy will work in cells, assuming UDP-5SGlcNAc (**4**) inhibits OGT.

To address whether UDP-5SGlcNAc (**4**) could act as an inhibitor of OGT we assessed its inhibitory activity using radiolabelled UDP-GlcNAc (**2**) as the sugar donor and nup62 as the acceptor. The amount of *O*-GlcNAc transferred was evaluated in the presence of increasing concentrations of UDP-5SGlcNAc (**4**). We found that UDP-5SGlcNAc (**4**) is an effective inhibitor of OGT with a K_i value of 8 μM (Supplementary Figure 1b), which means it binds as well as the natural substrate UDP-GlcNAc (**2**, K_m of between 2 and 7 μM)[33,35]. We also evaluated if inhibition of OGT by UDP-5SGlcNAc (**4**) occurred in a time-dependent manner by assessing activity following a 30 minute pre-incubation prior to addition of substrate. The rate of transfer of GlcNAc following pre-incubation of UDP-5SGlcNAc (**4**) with OGT or upon addition of the inhibitor at the same time as OGT were indistinguishable. In addition,

5SGlcNAc (**3**) was tested as an inhibitor of OGT, but no inhibition was observed at a concentration of 1 mM. These data strongly indicate the UDP moiety of UDP-5SGlcNAc (**4**) is critical for binding, and its biosynthesis from 5SGlcNAc (**3**) in cells is both feasible, based on the *in vitro* data, and essential for the non-covalent inhibition of OGT.

Effects of biosynthetic precursor 5SGlcNAc on cells

We next evaluated the effect of treating cells with 5SGlcNAc (**3**). Because peracetylated monosaccharides have been shown to enter cells more efficiently than their parent monosaccharides[22], we treated cultured COS-7 cells for 24 hours with 5SGlcNAc (**3**) or Ac-5SGlcNAc (**5**). As a control, to probe whether the presence of the acetyl groups contributed to any effects, we carried out experiments with 2-acetamido-1,3,4,6-tetra-*O*-acetyl-2-deoxy-α-D-glucopyranose (Ac-GlcNAc, **8**, Figure 1a) and did not observe any decreases in *O*-GlcNAc levels arising from treatment with this compound. Both 5SGlcNAc (**3**) and Ac-5SGlcNAc (**5**) decreased *O*-GlcNAc levels in a dose-dependent fashion as evaluated by western blots using an *O*-GlcNAc-directed antibody (CTD110.6) (Figure 2a and Supplementary Figures 6a-c). Treatment of cells with 50 μM UDP-5SGlcNAc (**4**) did not decrease *O*-GlcNAc levels (Supplementary Figure 6d), confirming UDP-5SGlcNAc (**4**) cannot itself effectively penetrate into cells.

To verify the utility of CTD110.6 in these assays we probed its ability to recognize both GlcNAc (**1**) and 5SGlcNAc (**3**) through blocking experiments. We found, however, by ^{1}H-NMR analysis that 5SGlcNAc (**3**) in D_2O exists predominantly as the α-anomer, making this compound inappropriate for blocking experiments to test antibodies that recognize *O*-GlcNAc. We therefore used the corresponding methyl glycosides; methyl 2-acetamido-2-deoxy-β-D-glucopyranoside (Me-GlcNAc, **9**, Figure 1a)[34] and methyl 2-acetamido-2-deoxy-5-thio-β-D-glucopyranoside (Me-5SGlcNAc, **10**, Figure 1a, see Supplementary Methods and Supplementary Scheme 3 for details of the synthesis and characterization). We found that Me-5SGlcNAc (**10**) did block binding, though not as well as Me-GlcNAc (**9**, Supplementary Figure 7a). Other commercial *O*-GlcNAc antibodies (RL2 and HGAC85) also revealed similar decreases in *O*-GlcNAc levels (Supplementary Figure 7b). These data support the interpretation that decreased *O*-GlcNAc levels arise from inhibition of OGT rather than from competitive accumulation of 5SGlcNAc (**3**) on proteins. Furthermore, given that *O*-GlcNAc is substoichiometric, often having ≤10% or lower site occupancy[36], 5SGlcNAc (**3**) would likely need to accumulate to dramatic levels on proteins in order to observe decreased *O*-GlcNAc levels. The lack of *O*-GlcNAc immunoreactivity observed when using Ac-5SGlcNAc (**5**) at higher doses is therefore most consistent with decreases in *O*-GlcNAc levels stemming from accumulation of UDP-5SGlcNAc (**4**) within cells and consequent inhibition of OGT.

Western blot analysis of the dose-dependent decreases in *O*-GlcNAc levels revealed the EC_{50} values for Ac-5SGlcNAc (**5**) and 5SGlcNAc (**3**) to be 5 μM and 700 μM, respectively, in COS-7 cells (Figure 2a and Supplementary Figures 6a-c for data and EC_{50} curves). Given the greater effectiveness of the acetylated precursor, we used Ac-5SGlcNAc (**5**) in all subsequent experiments. We also observed that treatment with Ac-5SGlcNAc (**5**) resulted in a time-dependent decrease in *O*-GlcNAc levels, with little *O*-GlcNAc being detectable after 24 hours (Figure 2b and Supplementary Figure 6e). Dosing of cells for five days showed *O*-GlcNAc levels dropped dramatically in the first day and subsequently remained low (Figure 2c). We evaluated some cellular responses to Ac-5SGlcNAc (**5**) treatment and consequent decreases in *O*-GlcNAc levels. In all studies and cell lines there were qualitatively no apparent changes in cell morphology or rate of proliferation at the doses assayed. We quantitatively evaluated cell proliferation and established growth curves over the course of 5 days in both CHO and EMEG32 heterozygous mouse embryonic fibroblast cells treated with

50 μM Ac-5SGlcNAc (**5**), 50 μM Ac-GlcNAc (**8**), or vehicle (Supplementary Figures 8a, b). For CHO cells the growth rate of Ac-5SGlcNAc (**5**) treated cells was indistinguishable from those of Ac-GlcNAc (**8**) and vehicle treated cells. In EMEG32 heterozygotes, the growth rates of the Ac-5SGlcNAc (**5**) and Ac-GlcNAc (**8**) treated cells were indistinguishable but were both lower than vehicle treated cells. The difference between vehicle and Ac-5SGlcNAc (**5**) or Ac-GlcNAc (**8**) treated cells likely stems from the effect of the acetyl groups; it is known that acetylated sugars can affect the growth rates of certain cell lines[22]. Interestingly, despite the absence of Ac-5SGlcNAc (**5**) specific effects on growth rate, clear decreases were observed in the levels of transcription factor Sp1. This observation is consistent with previous reports showing that knock-out of OGT and consequent decreases in *O*-GlcNAc levels, lead to a decrease in Sp1 levels[37] (Supplementary Figures 8c, d). Furthermore, while administration of Ac-GlcNAc (**8**) to cells had no effect, treatment with Ac-5SGlcNAc (**5**) induced a compensatory decrease in OGA levels and increase in OGT levels (Figure 2d and Supplementary Figure 9a), consistent with previous studies in which changes in *O*-GlcNAc levels lead to similar effects[10]. Notably, we found that although OGA levels continued to drop and OGT levels continued to rise over 5 days of dosing, *O*-GlcNAc levels remained consistently low and unchanged after 24 hours (Figure 2c and Supplementary Figure 9b). We observed that Ac-5SGlcNAc (**5**) treatment decreased *O*-GlcNAc levels uniformly within cells as evaluated using immunocytochemistry (Figure 2e). These observations together suggest that inhibition of OGT is highly efficient at the doses used in these assays. We next investigated the reversibility of the effect of Ac-5SGlcNAc (**5**) treatment and found that, following replacement of media with media containing no compound, *O*-GlcNAc returned to basal levels within 8 to 16 hours (Supplementary Figure 8e). To probe the generality of these effects, we also carried out a time course and dose response study in CHO cells (Supplementary Figures 10a-d). We noted similar temporal and dose response effects to those observed with COS-7 cells, though the EC_{50} value of 0.8 μM is six-fold lower. The five other cell lines we studied, including cultured fibroblasts, hepatocytes, and a differentiated neuronal model, all showed similar responses (Supplementary Figure 10e). These results collectively suggest the method should be general and widely applicable to many different cell types.

Effects of Ac-5SGlcNAc on an O-GlcNAc modified protein

We next probed *O*-GlcNAc levels on an individual protein after treatment with Ac-5SGlcNAc (**5**) by immunoprecipitating nup62 from cell lysates. nup62 is among the most heavily *O*-GlcNAc modified protein known, making it an interesting and useful test case[32,33]. To probe for *O*-GlcNAc on immunoprecipitated nup62 we used a commercial chemoenzymatic method[36] that involves chemoselective ligation of biotin to terminal GlcNAc residues. Chemoenzymatically labeled and unlabeled immunoprecipitated nup62 were both probed with streptavidin (Figure 3a and Supplementary Figure 11a); nup62 from untreated cells clearly shows *O*-GlcNAc modification, whereas nup62 derived from cells treated with Ac-5SGlcNAc (**5**) shows very little modification. An alternative approach to evaluating *O*-GlcNAc levels on nup62 that relies on band-shift assays has been described in the literature[23,32]. Previous observations reveal that nup62 can be observed as two bands under certain SDS-PAGE conditions; the upper band corresponds to *O*-GlcNAc modified nup62 whereas the lower band corresponds to a form of deglycosylated nup62[23,32]. We therefore analyzed immunoprecipitated nup62 in this way and found, as expected, that nup62 from untreated cells appeared only as the upper band in western blots and this species was heavily *O*-GlcNAc modified (Figure 3b and Supplementary Figure 11b). Treating this *O*-GlcNAc modified nup62 precipitate with a bacterial homologue of OGA (*Bt*GH84[38]) greatly diminished *O*-GlcNAc immunoreactivity and the resulting deglycosylated nup62 appeared, as expected, as the lower band. This is precisely what has been observed previously[23,32]. A different scenario is observed when analyzing nup62 from cells treated

with Ac-5SGlcNAc (**5**). In a dose-dependent manner, nup62 appears as a doublet of bands by western blot (Figure 3c and Supplementary Figure 11c). To address the *O*-GlcNAc modification state of these two bands, we immunoprecipitated nup62 from cells treated with Ac-5SGlcNAc (**5**) and analyzed the resulting samples (Figure 3b and Supplementary Figure 11b). The results verify that nup62 is a mixture of two species when OGT is inhibited; an upper band, which appears partially *O*-GlcNAc modified, and a lower band, which is a form of nup62 that essentially lacks *O*-GlcNAc (Figure 3b and Supplementary Figure 11b). *Bt*GH84-mediated removal of *O*-GlcNAc from this immunoprecipitated nup62 sample derived from Ac-5SGlcNAc (**5**) treated cells resulted in near complete loss of remaining *O*-GlcNAc immunoreactivity and only the lower band was observed when probed for nup62. This observation is consistent with any remaining *O*-GlcNAc on the partly modified upper band of nup62 from Ac-5SGlcNAc (**5**) treated cells being removed by *Bt*GH84. Therefore, Ac-5SGlcNAc (**5**) dramatically decreases *O*-GlcNAc levels on all proteins observable by western blot (Figure 2a), even on proteins such as nup62 that are constitutively and heavily *O*-GlcNAc modified in cells.

Metabolic feeding of 5SGlcNAz

The collective observations described above revealed that *O*-GlcNAc modification of substrate proteins is decreased by Ac-5SGlcNAc (**5**) treatment and strongly indicate it is unlikely that 5SGlcNAc (**3**) is being incorporated onto proteins. However, to further probe this possibility, we used a metabolic feeding and chemoselective ligation strategy. It is known that 2-azidoacetamido-2-deoxy-D-glucopyranose (GlcNAz, **11**, Figure 4a) can be assimilated by the HBP to form uridine diphospho-*N*-azidoacetylglucosamine (UDP-GlcNAz, **12**, Figure 4a) and then be installed onto proteins as *O*-GlcNAz[23]. Using a chemoselective ligation to install a reporter group allows sensitive detection of *O*-GlcNAz modified proteins[23]. By analogy, we reasoned that we could evaluate whether 2-azidoacetamido-2-deoxy-5-thio-D-glucopyranose (5SGlcNAz, **13**, Figure 4a) is incorporated onto proteins and that this would inform on whether 5SGlcNAc (**3**) might be transferred onto proteins in cells. This approach has the advantage that it relies on neither recognition of potential *O*-5SGlcNAc by the three antibodies tested nor by the GalT used for the chemoenzymatic labelling approach. We therefore carried out the synthesis of 1,3,4,6-tetra-*O*-acetyl-2-azidoacetamido-2-deoxy-5-thio-α-D-glucopyranose (Ac-5SGlcNAz, **14**, Figure 4a) in 15 steps, the last two steps of which diverge from a previously known compound[39] (see Supplementary Methods, Supplementary Scheme 4, and Supplementary Figure 12 for details of the synthesis and characterization). Briefly, these two steps involved catalytic hydrogenation followed by DCC coupling, and furnished Ac-5SGlcNAz (**14**) in reasonable yield. Treating cells with either vehicle, 1,3,4,6-tetra-*O*-acetyl-2-azidoacetamido-2-deoxy-α-D-glucopyranose[23] (**15**, Ac-GlcNAz, Figure 4a) or Ac-5SGlcNAz (**14**) revealed that only 5SGlcNAz (**13**) decreased *O*-GlcNAc levels (Figure 4b). Proteins from cells treated with vehicle, Ac-GlcNAz (**15**), or Ac-5SGlcNAz (**14**) were collected and subjected to Staudinger ligation[40] with biotin phosphine (Figure 4a). Following the ligation, proteins were blotted onto nitrocellulose and probed using streptavidin-horse radish peroxidase. Only proteins from cells treated with Ac-GlcNAz (**15**) revealed any signal, whereas the signal from cells treated with vehicle were indistinguishable from those treated with Ac-5SGlcNAz (**14**) (Figure 4b). Similarly, we immunoprecipitated nup62 from cells treated with vehicle, Ac-GlcNAz (**15**), or Ac-5SGlcNAz (**14**), and prior to Staudinger ligation, incubated half of each sample with *Bt*GH84[38]. The resulting blot, probed with streptavidin-HRP, once again only showed signal from nup62 immunoprecipitated from cells treated with Ac-GlcNAz (**15**), and only in the sample that had not been subjected to *Bt*GH84 hydrolysis (Figure 4c and Supplementary Figure 13). The observation that Ac-5SGlcNAz (**14**) greatly decreases *O*-GlcNAc levels strongly indicates that uridine diphospho-5-thio-*N*-azidoacetylglucosamine (UDP-5SGlcNAz, **16**, Figure 4a) is formed within cells where it acts to inhibit OGT. The

chemoselective ligation data, however, indicates that 5SGlcNAz (**13**) does not accumulate on proteins to any measurable level. These data, in combination with the studies described above, provide strong evidence that 5SGlcNAc (**3**) does not accumulate on proteins, and that decreased *O*-GlcNAc levels arise from inhibition of OGT by UDP-5SGlcNAc (**4**).

Assessing cellular levels of UDP-sugar pools

An alternate process, aside from inhibition of OGT by UDP-5SGlcNAc (**4**), which could cause decreased *O*-GlcNAc levels in cells treated with Ac-5SGlcNAc (**5**) is that the pool of UDP-GlcNAc (**2**) in cells might be greatly diminished. To verify that UDP-5SGlcNAc (**4**) is being biosynthesized within cells, and to evaluate the relative levels of UDP-GlcNAc (**2**) and other nucleotide sugar donors within cells, we treated COS-7 cells with different concentrations of Ac-5SGlcNAc (**5**). Analysis of the extracted UDP-sugars using CE (Figures 5a, b, and Supplementary Figures 14a, b) revealed a dose dependent increase in the amount of UDP-5SGlcNAc (**4**) in cells and a statistically significant decrease in UDP-GlcNAc (**2**) (p=0.022; n=3) and UDP-GalNAc (p=0.022; n=3) levels. An additional peak corresponding to a synthetic standard of UDP-5SGalNAc is also observed (Supplementary Figures 14a, c), while UDP-Glc and UDP-Gal levels are unaffected. The accumulation of UDP-5SGlcNAc (**4**) is consistent with this compound being a poor substrate for OGT. Notably, when we treated cells with 50 μM Ac-5SGlcNAc (**5**), which is a concentration well above the EC_{50} value and at which we found near complete loss of *O*-GlcNAc in all cell lines tested (Figure 2a and Supplementary Figures 6a and 10a, b, e), we observed that UDP-GlcNAc (**2**) levels are still more than 60% of basal levels. This decrease in UDP-GlcNAc (**2**) levels is highly unlikely to account for the low *O*-GlcNAc levels observed in treated cells. These observations therefore support the view that 5SGlcNAc (**3**) can efficiently traverse the HBP to form levels of UDP-5SGlcNAc (**4**) that proficiently inhibit OGT in cells.

Effect of Ac-5SGlcNAc on cell surface glycosylation

The modest decrease in UDP-GlcNAc (**2**) levels and accumulation of UDP-5SGlcNAc (**4**) within cells observed upon Ac-5SGlcNAc (**5**) treatment prompted us to consider that cell surface glycosylation could be affected through changes in either UDP-GlcNAc (**2**) availability or inhibition of various GlcNAc transferases within the secretory pathway. To assess this possibility we treated COS-7 cells with a range of Ac-5SGlcNAc (**5**) concentrations and evaluated the effect on various glycans by lectin blot analysis. All lectins tested showed no changes in glycosylation of cellular proteins, even at the highest doses of Ac-5SGlcNAc (**5**) assayed (Figure 6a and Supplementary Figure 15a). These lectins probe for both high mannose (ConA and GNA) and complex *N*-glycans (PHA-L, SNA, and MAA). We also examined the effect of Ac-5SGlcNAc (**5**) on *N*-glycosylation of an individual protein by taking advantage of the high level production of IgG from mouse hybridoma cell lines. We found that immunoprecipitated IgG from a hybridoma cell line appeared to possess only high mannose glycans. Analysis of the glycosylation of this IgG using appropriate lectins, GNA and ConA, revealed only a slight decrease in immunoreactivity when the very highest (1000 μM) dose of Ac-5SGlcNAc (**5**) was used (Figure 6b and Supplementary Figure 15b). These collective observations are consistent with reports showing that EMEG32$^{-/-}$ cells, which are deficient in the biosynthesis of GlcNAc (**1**), have very low UDP-GlcNAc (**2**) levels but *N*-glycosylation is virtually unaffected[41]. Within EMEG32$^{-/-}$ cells it appears that ~5% of the normal UDP-GlcNAc (**2**) recovered by salvage pathways is sufficient to sustain *N*-glycosylation[41], as measured in the same way we evaluate *N*-glycosylation here. In this regard, our results are consistent with the EMEG32$^{-/-}$ studies since the low levels of UDP-GlcNAc (**2**) observed in EMEG32$^{-/-}$

cells are much lower than those observed when using concentrations of Ac-5SGlcNAc (**5**) that effectively decrease *O*-GlcNAc levels.

Discussion

Here we describe a Trojan horse strategy to generating a GT inhibitor that acts in cells. We found that the metabolic precursors 5SGlcNAc (**3**) and Ac-5SGlcNAc (**5**) can be processed both *in vitro* and in cells by the mammalian enzymes of the GlcNAc salvage pathway and the hexosamine biosynthetic pathway to generate UDP-5SGlcNAc (**4**). Several lines of evidence strongly support the view that UDP-5SGlcNAc (**4**) neither serves as an efficient substrate for OGT nor does 5SGlcNAc accumulate on proteins. Instead, formation of UDP-5SGlcNAc (**4**) within cells inhibits OGT function and leads to decreased cellular *O*-GlcNAc levels. All cell lines assayed show similar responses, consistent with conservation of both the HBP and OGT within different mammals. Interestingly, UDP-5SGlcNAc (**4**) shows cell line specific EC_{50} values for reduction of *O*-GlcNAc levels in the single digit μM range, however, we found that there was no apparent interference with cell surface glycosylation over the time frames tested, as probed using various lectins. It should be noted, however, that the absence of any apparent effect on cell surface glycosylation measured in this way does not indicate whether or not UDP-5SGlcNAc is selective for OGT. It is likely that *O*-GlcNAc cycling occurs more rapidly than recycling and presentation of cell surface glycans, and this difference could account for the observation that *O*-GlcNAc levels decrease while cell surface glycosylation appears unchanged. Furthermore, it is also possible that 5SGlcNAc (**3**) does not partition between the cytosol and the secretory pathway in the same way as GlcNAc (**1**) and this could contribute to the apparent differential effects on secretory glycosyltransferases as compared to OGT. Interestingly, we also found that Ac-5SGlcNAc (**5**) induced abrogation of *O*-GlcNAc in two different cell lines showed no apparent compound specific toxicity and did not affect cellular growth rates. This last observation is in contrast to genetic studies that show loss or knock-down of OGT, and consequent loss of *O*-GlcNAc, cripples cellular proliferation. This discrepancy may stem from the rapid and dramatic changes in OGT levels induced by its over-expression or knock-down. Indeed, OGT is a large protein with many partners, and such changes might alter the levels of critical protein complexes. Alternatively, it may be that the cycling of *O*-GlcNAc is important. In any case, the results we observed suggest that greatly diminished *O*-GlcNAc levels do not impair cellular proliferation. Further studies will be needed to clarify the precise basis for the differences observed when carrying out genetic or chemical intervention. Regardless, the utility of Ac-5SGlcNAc (**5**), and the apparent lack of toxicity associated with this molecule, should make this a valuable tool for studying the effects of decreased *O*-GlcNAc levels on cellular processes.

More generally, previously described rational approaches to inhibition of GTs include the use of acceptor substrate decoys to ‘distract’ GTs from their natural substrates[42], as well as metabolic feeding approaches to generate dead-end acceptor substrate mimics[43]. Recently, an intriguing new approach was described in which chemical modification of the uridine base of uridine diphosphogalactose (UDP-Gal) resulted in a compound that was turned over by galactosyltransferases much more slowly than UDP-Gal. The compound acted as an inhibitor *in vitro* and it remains to be tested in cells and tissues[44]. To our best knowledge, however, there have been no examples of rationally designed inhibitors that emulate a natural nucleotide sugar donor substrate and act in cells. Indeed, there are strikingly few examples of GT inhibitors that work in cells and these are natural products, serendipitously discovered synthetic compounds, or compounds identified through high-throughput screening[2,11,45,46]. To address this issue we were stimulated by the demonstrated tolerance of nucleotide sugar biosynthetic pathways for the introduction of unnatural monosaccharides into glycans, to consider a new approach to inhibition of GTs within cells. Here we find this

strategy circumvents problems associated with the poor cell permeability of many current rationally designed GT inhibitors that already incorporate anionic groups. One attractive future prospect being actively pursued is that by using this strategy of biosynthetic precursor delivery we envision that it may be feasible to generate a panel of GT inhibitors that could catalyze the study of the biological roles of a variety of GTs. In this regard such probes might serve as a starting point for designing inhibitors of GTs that are drug targets for various diseases including, for example, diabetes[7], inflammation[3], and cancer[4].

Methods

Synthesis of 5SGlcNAc (3), Ac-5SGlcNAc (5), pMP-5SGlcNAc (7), Me-5SGlcNAc (10), and Ac-5SGlcNAz (14)

Synthesis of 5SGlcNAc (**3**) and Ac-5SGlcNAc (**5**) was performed as described previously[31] with some minor modifications. Synthesis of *p*MP-5SGlcNAc (**7**) and Me-5SGlcNAc (**10**) were carried out using a trichloroacetimidiate donor as the key intermediate. Synthesis of Ac-5SGlcNAz (**14**) was carried out over 15 steps, diverging from an established synthesis[39] for the final two steps. A full description of the methods used and characterization of the compounds are provided in the Supplementary Methods.

Chemoenzymatic synthesis of UDP-5SGlcNAc (4)

Over-expression and purification of GNK, AGM, and AGX1 were carried out as described previously[47-49]. Details regarding the enzymatic synthesis can be found in the Supplementary Methods.

Purification of UDP-5SGlcNAc (4)

The UDP-5SGlcNAc (**4**) product was isolated using a procedure described for other UDP-sugars with minor modifications as reported in the Supplementary Methods.

Capillary electrophoresis (CE)

CE was performed on a ProteomeLab PA800 (Beckman-Coulter) using fused silica capillaries of 50 μM internal diameter × 44 cm (to detector). Further details can be found in the Supplementary Methods.

OGT transfer

The ability of OGT (over-expressed and purified as described in Ref. [35]) to transfer UDP-5SGlcNAc (**4**) was tested using recombinant nup62 as the acceptor. Further details can be found in the Supplementary Methods.

OGT inhibition

The ability of 5SGlcNAc (**3**) and UDP-5SGlcNAc (**4**) to inhibit OGT activity was assessed using radiolabelled UDP-[^{3}H]-GlcNAc (American Radiolabel) as the donor and recombinant nup62 as the acceptor. Assays were carried out essentially as described previously[35] and the K_i determined by Dixon analysis. Further details can be found in the Supplementary Methods.

Cell culture

Cell lines and culture conditions were: COS-7, Dulbecco's modified Eagle's medium (DMEM, Invitrogen)/5% fetal bovine serum (FBS, Invitrogen); HepG2, SK-N-SH, EMEG32$^{+/-}$ and EMEG32$^{-/-}$, DMEM/5% FBS; CHO, DMEM/F-12/5-10% FBS; and PC12 cells, DMEM/5% FBS and 5% horse serum. PC12 cells were plated at a density of 3-4 × 10^5

cells/10 cm plate (pre-treated with 5 μg/cm^2 rat tail collagen (BD Biosciences)) and differentiated as described previously[12]. Mouse hybridoma cells (Developmental Studies Hybridoma Bank; antibody E7 for β-tubulin) were cultured in RPMI40/10% FBS. Upon treatment of hybridoma cells with Ac-5SGlcNAc (**5**), the media was changed to serum free RPMI40. Following treatment with 5SGlcNAc (**3**), UDP-5SGlcNAc (**4**) or Ac-5SGlcNAc (**5**), cells were harvested by gentle washing with PBS, lysed in SDS loading buffer, and boiled for 10 minutes. To collect IgG the cells were pelleted (800 x g, 5 min) and IgG was precipitated from the supernatant (see below for details).

Western/lectin blots

Samples were analyzed using standard procedures as described in the Supplementary Methods. Densitometry was performed using ImageQuant 5.2 (Molecular Dynamics) and fits to the data were made using GRAFIT.

Antibodies/lectins

A list of antibodies and lectins are provided in the Supplementary Methods.

Immunocytochemistry

Details are provided in the Supplementary Methods.

Blocking antibody interactions

Modified nup62 was electrophoresed through a gel and transferred onto nitrocellulose membrane. CTD110.6 at the appropriate dilution was mixed with 0-3 mM Me-GlcNAc (**9**) or Me-5SGlcNAc (**10**) for 1 h prior to incubation with the membrane overnight at 4 °C. The standard procedure for western blots was subsequently followed.

OGA kinetics

Kinetics were performed at 37 °C in phosphate buffered saline (PBS), pH 7.4, in a total volume of 150 μL. Substrate concentrations of 25 μM to 1.5 mM were used for *p*MP-GlcNAc (**6**) and 25 to 800 μM for *p*MP-5SGlcNAc (**7**). OGA (which was over-expressed and purified as described in Ref. [50]) was used at a concentration of 1 μM for *p*MP-GlcNAc (**6**) and 3.6 μM for *p*MP-5SGlcNAc (**7**). Rates were monitored at a wavelength of 296 nm over the course of 10-20 min. Data were fit to the Michaelis-Menten equation using GRAFIT and the k_{cat} and K_M values determined.

Cell growth curves

Details are provided in the Supplementary Methods.

Immunoprecipitation of nup62

nup62 was immunoprecipitated from COS-7 cell lysates using the procedure described in Ref. [23]. Following washing of the beads, and prior to elution, nup62 was incubated in the absence or presence of *Bt*GH84 (overexpressed and purified as described previously[38]) with shaking for 2 h at room temperature. The beads were washed three times with PBS and nup62 was subsequently eluted from the beads by addition of SDS loading buffer and boiling for 10 min.

Treatment with Ac5SGlcNAz

Following treatment with Ac5SGlcNAz (**14**), cells were harvested by gentle washing with PBS, lysed by sonication in PBS containing 0.5% NP-40 and centrifuged to remove any insoluble material. Cell lysates were incubated with biotinylated phosphine in 20% DMF, at

a final concentration of 200 μM, and incubated at 37 °C for 2 h. SDS loading buffer was added to the samples and they were boiled for 5 min.

Click-iT® kit for labelling O-GlcNAc residues

The 'Click-iT® *O*-GlcNAc Enzymatic Labeling System' was purchased from Invitrogen, and the manufacturer's protocol was followed with some alterations as reported in the Supplementary Methods.

Extraction of nucleotide sugars from cell lysates

COS-7 cells were treated with Ac-5SGlcNAc (**5**, 0 to 1000 μM) for 24 h in triplicate. Cell supernatants from lysed cells were prepared, frozen, and lyophilized. The nucleotide sugar extraction protocol is described in the Supplementary Methods.

Precipitation of antibody

Conditioned serum free media from mouse hybridoma cell cultures was incubated with 100 μL Protein G/Protein-A agarose beads (Calbiochem) with shaking overnight at 4 °C. Beads were washed three times in PBS containing 0.1% NP-40. Antibody was eluted by the addition of SDS-PAGE loading buffer and boiling for 10 min. Western blots were probed with secondary goat anti-mouse IgG antibody (using the western blot procedure described in the Supplementary Methods, starting from the second blocking step).

PNGase F cleavage

PNGase F was purchased from New England Biolabs and used as described in the manufacturer's protocol for cell lysates. Immunoprecipitated antibody (from hybridoma cells) was eluted from the beads using 1% SDS and then underwent PNGase F cleavage in the same buffer.

Supplementary Material

Refer to Web version on PubMed Central for supplementary material.

Acknowledgments

The plasmid encoding GNK was a kind gift from Dr. Markus Berger and Dr. Stephan Hinderlich, and the plasmid encoding AGX1 was a kind gift from Dr. Veronique Piller. Polyclonal anti-OGA antibody was a kind gift from Dr. Gerald Hart. We thank Dr. Gideon Davies for the *E. coli* expression construct of *Bt*GH84. T.M.G. is a Sir Henry Wellcome postdoctoral fellow and a Michael Smith for Health Research (MSFHR) trainee award holder. D.J.V. is a scholar of the MSFHR and holds a Canada Research Chair in Chemical Glycobiology. The Natural Sciences and Engineering Research Council of Canada and Simon Fraser University are thanked for funding support.

References

1. Varki, A.; Lowe, JB. Biological roles of glycans. In: Varki, A., et al., editors. Essentials of Glycobiology. CSH Press; 2009.
2. Platt FM, Neises GR, Dwek RA, Butters TD. N-butyldeoxynojirimycin is a novel inhibitor of glycolipid biosynthesis. J Biol Chem. 1994; 269:8362–8365. [PubMed: 8132559]
3. Lowe JB. Glycan-dependent leukocyte adhesion and recruitment in inflammation. Curr Opin Cell Biol. 2003; 15:531–538. [PubMed: 14519387]
4. Granovsky M, et al. Suppression of tumor growth and metastasis in Mgat5-deficient mice. Nat Med. 2000; 6:306–312. [PubMed: 10700233]
5. Hart GW, Housley MP, Slawson C. Cycling of *O*-linked beta-*N*-acetylglucosamine on nucleocytoplasmic proteins. Nature. 2007; 446:1017–1022. [PubMed: 17460662]

6. Roquemore EP, Chevrier MR, Cotter RJ, Hart GW. Dynamic O-GlcNAcylation of the small heat shock protein alpha B-crystallin. Biochemistry. 1996; 35:3578–3586. [PubMed: 8639509]
7. Yang X, et al. Phosphoinositide signalling links O-GlcNAc transferase to insulin resistance. Nature. 2008; 451:964–969. [PubMed: 18288188]
8. Sinclair DA, et al. Drosophila O-GlcNAc transferase (OGT) is encoded by the Polycomb group (PcG) gene, super sex combs (sxc). Proc Natl Acad Sci USA. 2009; 106:13427–13432. [PubMed: 19666537]
9. Zachara NE, et al. Dynamic O-GlcNAc modification of nucleocytoplasmic proteins in response to stress. A survival response of mammalian cells. J Biol Chem. 2004; 279:30133–30142. [PubMed: 15138254]
10. Slawson C, et al. Perturbations in O-linked β-N-acetylglucosamine protein modification cause severe defects in mitotic progression and cytokinesis. J Biol Chem. 2005; 280:32944–32956. [PubMed: 16027160]
11. Caldwell SA, et al. Nutrient sensor O-GlcNAc transferase regulates breast cancer tumorigenesis through targeting of the oncogenic transcription factor FoxM1. Oncogene. 2010; 29:2831–2842. [PubMed: 20190804]
12. Yuzwa SA, et al. A potent mechanism-inspired *O*-GlcNAcase inhibitor that blocks phosphorylation of tau *in vivo*. Nat Chem Biol. 2008; 4:483–490. [PubMed: 18587388]
13. Liu F, Iqbal K, Grundke-Iqbal I, Hart GW, Gong CX. O-GlcNAcylation regulates phosphorylation of tau: a mechanism involved in Alzheimer's disease. Proc Natl Acad Sci USA. 2004; 101:10804–10809. [PubMed: 15249677]
14. Liu J, Marchase RB, Chatham JC. Increased O-GlcNAc levels during reperfusion lead to improved functional recovery and reduced calpain proteolysis. Am J Physiol Heart Circ Physiol. 2007; 293:H1391–1399. [PubMed: 17573462]
15. Ngoh GA, Hamid T, Prabhu SD, Jones SP. O-GlcNAc signaling attenuates ER stress-induced cardiomyocyte death. Am J Physiol Heart Circ Physiol. 2009; 297:H1711–1719. [PubMed: 19734355]
16. Lyons SD, Sant ME, Christopherson RI. Cytotoxic mechanisms of glutamine antagonists in mouse L1210 leukemia. J Biol Chem. 1990; 265:11377–11381. [PubMed: 2358467]
17. Lenzen S, Panten U. Alloxan: history and mechanism of action. Diabetologia. 1988; 31:337–342. [PubMed: 3046975]
18. Gross BJ, Kraybill BC, Walker S. Discovery of *O*-GlcNAc transferase inhibitors. J Am Chem Soc. 2005; 127:14588–14589. [PubMed: 16231908]
19. Ngoh GA, Watson LJ, Facundo HT, Dillmann W, Jones SP. Non-canonical glycosyltransferase modulates post-hypoxic cardiac myocyte death and mitochondrial permeability transition. J Mol Cell Cardiol. 2008; 45:313–325. [PubMed: 18539296]
20. Keppler OT, Horstkorte R, Pawlita M, Schmidt C, Reutter W. Biochemical engineering of the N-acyl side chain of sialic acid: biological implications. Glycobiology. 2001; 11:11R–18R. [PubMed: 11181557]
21. Agard NJ, Bertozzi CR. Chemical approaches to perturb, profile, and perceive glycans. Acc Chem Res. 2009; 42:788–797. [PubMed: 19361192]
22. Jones MB, et al. Characterization of the cellular uptake and metabolic conversion of acetylated N-acetylmannosamine (ManNAc) analogues to sialic acids. Biotechnol Bioeng. 2004; 85:394–405. [PubMed: 14755557]
23. Vocadlo DJ, Hang HC, Kim EJ, Hanover JA, Bertozzi CR. A chemical approach for identifying O-GlcNAc-modified proteins in cells. Proc Natl Acad Sci USA. 2003; 100:9116–9121. [PubMed: 12874386]
24. Lairson LL, Henrissat B, Davies GJ, Withers SG. Glycosyltransferases: structures, functions, and mechanisms. Annu Rev Biochem. 2008; 77:521–555. [PubMed: 18518825]
25. Yuasa H, Izumi M, Hashimoto H. Thiasugars: potential glycosidase inhibitors. Curr Top Med Chem. 2009; 9:76–86. [PubMed: 19199997]
26. Tsuruta O, Shinohara G, Yuasa H, Hashimoto H. UDP-*N*-acetyl-5-thio-galactosamine is a substrate of lactose synthase. Bioorg Med Chem Lett. 1997; 7:2523–2526.

27. Tsuruta O, et al. Synthesis of GDP-5-thiosugars and their use as glycosyl donor substrates for glycosyltransferases. J Org Chem. 2003; 68:6400–6406. [PubMed: 12895077]
28. Offen W, et al. Structure of a flavonoid glucosyltransferase reveals the basis for plant natural product modification. EMBO J. 2006; 25:1396–1405. [PubMed: 16482224]
29. Lambert JB, Wharry SM. Conformational-Analysis of 5-Thio-D-Glucose. J Org Chem. 1981; 46:3193–3196.
30. Zhao G, Guan W, Cai L, Wang PG. Enzymatic route to preparative-scale synthesis of UDP-GlcNAc/GalNAc, their analogues and GDP-fucose. Nat Protoc. 5:636–646. [PubMed: 20224564]
31. Tanahashi E, Kiso T, Hasegawa A. A facile synthesis of 2-acetamido-2-deoxy-5-thio-D-glucopyranose. Carbohydr Res. 1983; 117:304–308.
32. Davis LI, Blobel G. Nuclear pore complex contains a family of glycoproteins that includes p62: glycosylation through a previously unidentified cellular pathway. Proc Natl Acad Sci USA. 1987; 84:7552–7556. [PubMed: 3313397]
33. Lubas WA, Smith M, Starr CM, Hanover JA. Analysis of nuclear pore protein p62 glycosylation. Biochemistry. 1995; 34:1686–1694. [PubMed: 7849028]
34. Greig IR, Macauley MS, Williams IH, Vocadlo DJ. Probing synergy between two catalytic strategies in the glycoside hydrolase O-GlcNAcase using multiple linear free energy relationships. J Am Chem Soc. 2009; 131:13415–13422. [PubMed: 19715310]
35. Martinez-Fleites C, et al. Structure of an O-GlcNAc transferase homolog provides insight into intracellular glycosylation. Nat Struct Mol Biol. 2008; 15:764–765. [PubMed: 18536723]
36. Khidekel N, et al. Probing the dynamics of O-GlcNAc glycosylation in the brain using quantitative proteomics. Nat Chem Biol. 2007; 3:339–348. [PubMed: 17496889]
37. O'Donnell N, Zachara NE, Hart GW, Marth JD. Ogt-dependent X-chromosome-linked protein glycosylation is a requisite modification in somatic cell function and embryo viability. Mol Cell Biol. 2004; 24:1680–1690. [PubMed: 14749383]
38. Dennis RJ, et al. Structure and mechanism of a bacterial beta-glucosaminidase having O-GlcNAcase activity. Nat Struct Mol Biol. 2006; 13:365–371. [PubMed: 16565725]
39. Csuk R, Glanzer BI. A short synthesis of 2-acetamido-2-deoxy-5-thio-D-glucose and D-mannose from 5-thio-glucal. J Chem Soc Chem Comm. 1986:343–344.
40. Saxon E, Bertozzi CR. Cell surface engineering by a modified Staudinger reaction. Science. 2000; 287:2007–2010. [PubMed: 10720325]
41. Boehmelt G, et al. Decreased UDP-GlcNAc levels abrogate proliferation control in EMeg32-deficient cells. EMBO J. 2000; 19:5092–5104. [PubMed: 11013212]
42. Sarkar AK, Fritz TA, Taylor WH, Esko JD. Disaccharide uptake and priming in animal cells: inhibition of sialyl Lewis X by acetylated Gal beta 1→4GlcNAc beta-O-naphthalenemethanol. Proc Natl Acad Sci USA. 1995; 92:3323–3327. [PubMed: 7724561]
43. Ralton JE, Milne KG, Guther ML, Field RA, Ferguson MA. The mechanism of inhibition of glycosylphosphatidylinositol anchor biosynthesis in Trypanosoma brucei by mannosamine. J Biol Chem. 1993; 268:24183–24189. [PubMed: 8226965]
44. Pesnot T, Jorgensen R, Palcic MM, Wagner GK. Structural and mechanistic basis for a new mode of glycosyltransferase inhibition. Nat Chem Biol. 2010; 6:321–323. [PubMed: 20364127]
45. Lee KY, et al. The hexapeptide inhibitor of Galβ1,3GalNAc-specific α2,3-sialyltransferase as a generic inhibitor of sialyltransferases. J Biol Chem. 2002; 277:49341–49351. [PubMed: 12379642]
46. Schneider EG, Nguyen HT, Lennarz WJ. The effect of tunicamycin, an inhibitor of protein glycosylation, on embryonic development in the sea urchin. J Biol Chem. 1978; 253:2348–2355. [PubMed: 632274]
47. Hinderlich S, Berger M, Schwarzkopf M, Effertz K, Reutter W. Molecular cloning and characterization of murine and human N-acetylglucosamine kinase. Eur J Biochem. 2000; 267:3301–3308. [PubMed: 10824116]
48. Mio T, Yamada-Okabe T, Arisawa M, Yamada-Okabe H. Functional cloning and mutational analysis of the human cDNA for phosphoacetylglucosamine mutase: identification of the amino acid residues essential for the catalysis. Biochim Biophys Acta. 2000; 1492:369–376. [PubMed: 11004509]

49. Bourgeaux V, Piller F, Piller V. Two-step enzymatic synthesis of UDP-N-acetylgalactosamine. Bioorg Med Chem Lett. 2005; 15:5459–5462. [PubMed: 16203137]

50. Macauley MS, Stubbs KA, Vocadlo DJ. O-GlcNAcase catalyzes cleavage of thioglycosides without general acid catalysis. J Am Chem Soc. 2005; 127:17202–17203. [PubMed: 16332065]

Europe PMC Funders Author Manuscripts

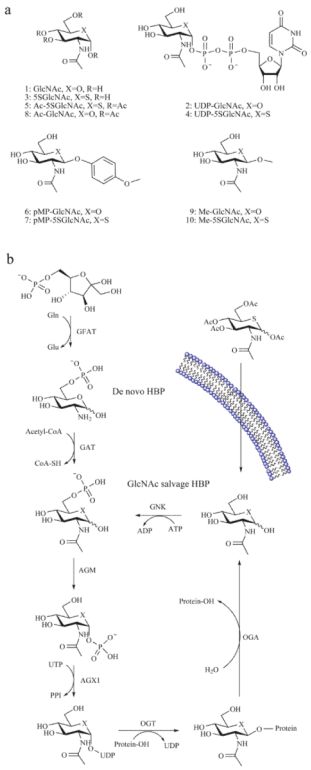

Figure 1. The mammalian hexosamine biosynthetic pathway (HBP), GlcNAc salvage pathway, and the structures of compounds studied here

(a) Structures of some of the molecules used in this study (X = O or S as indicated, R = H or Ac as indicated). (b) The end product of the HBP is UDP-GlcNAc (**2**), the donor substrate used by OGT. The first step in the *de novo* pathway, where fructose-6-phosphate is converted to glutamine-6-phosphate, is catalyzed by glutamine: fructose-6-phosphate amidotransferase (GFAT). Glutamine-6-phosphate is transformed into GlcNAc-6-phosphate by acetyl-CoA:D-glucosamine-6-phosphate *N*-acetyltransferase (GAT). The GlcNAc salvage pathway recycles cellular GlcNAc (**1**), which is converted into GlcNAc-6-phosphate by GlcNAc kinase (GNK). GlcNAc-6-phosphate is converted into GlcNAc-1-phosphate by GlcNAc mutase (AGM), and then to the end product, UDP-GlcNAc, by UDP-GlcNAc pyrophosphorylase (AGX1). The endocyclic heteroatom is denoted X (O in nature and S in the synthetic compounds depicted in panel a). 5SGlcNAc (**3**) is converted *via* the salvage pathway to generate intracellular UDP-5SGlcNAc (**4**). Ac-5SGlcNAc (**5**) is deacetylated by cellular esterases.

Europe PMC Funders Author Manuscripts

Europe PMC Funders Author Manuscripts

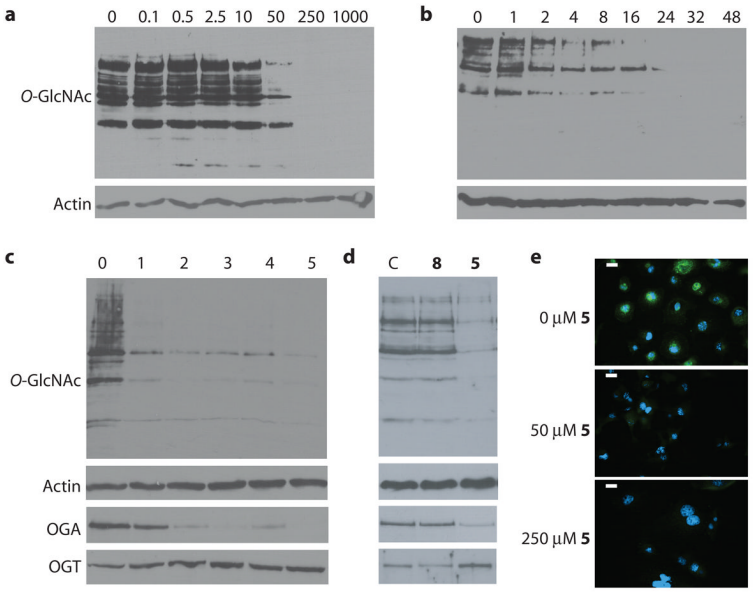

Figure 2. Ac-5SGlcNAc (5) acts in cells to decrease global *O*-GlcNAc levels in a dose and time dependent manner

(a) Western blots of COS-7 cell lysates following Ac-5SGlcNAc (**5**) administration at different doses (0-1000 μM) for 24 h. Upper panel, probed with anti-*O*-GlcNAc antibody (CTD110.6); lower panel, probed with anti-actin antibody. Densitometry analysis (see Supplementary Figure 6a) yields an EC_{50} value of 5 μM. (b) Western blots of COS-7 cell lysates following Ac-5SGlcNAc (**5**) administration at 50 μM for various times. Upper panel, probed with CTD110.6; lower panel, probed with anti-actin antibody. Densitometry analysis (see Supplementary Figure 6e) shows how *O*-GlcNAc levels diminish over time. (c) Western blots of COS-7 cell lysates following Ac-5SGlcNAc (**5**) administration at 50 μM for different amounts of time. Probed with (from top to bottom) anti-*O*-GlcNAc antibody (CTD110.6), anti-OGA antibody, anti-OGT antibody, and anti-actin antibody. Full versions of the blots are shown in Supplementary Figure 9b. (d) Western blots of COS-7 cell lysates administered specified agents at 50 μM for 24 h; vehicle only (C), Ac-GlcNAc (**8**) or Ac-5SGlcNAc (**5**). Probed with (from top to bottom) anti-*O*-GlcNAc antibody (CTD110.6), anti-OGA antibody, anti-OGT antibody, and anti-actin antibody. Full versions of the blots are shown in Supplementary Figure 9a. (e) Immunocytochemistry of COS-7 cells treated with no, 50 μM or 250 μM Ac-5SGlcNAc (**5**) for 24 hours. Immunoreactivity from anti-*O*-GlcNAc antibody CTD110.6 is shown in green and DAPI (which stains DNA in the nucleus) in blue. The white bar corresponds to a distance of 25 μM.

Europe PMC Funders Author Manuscripts

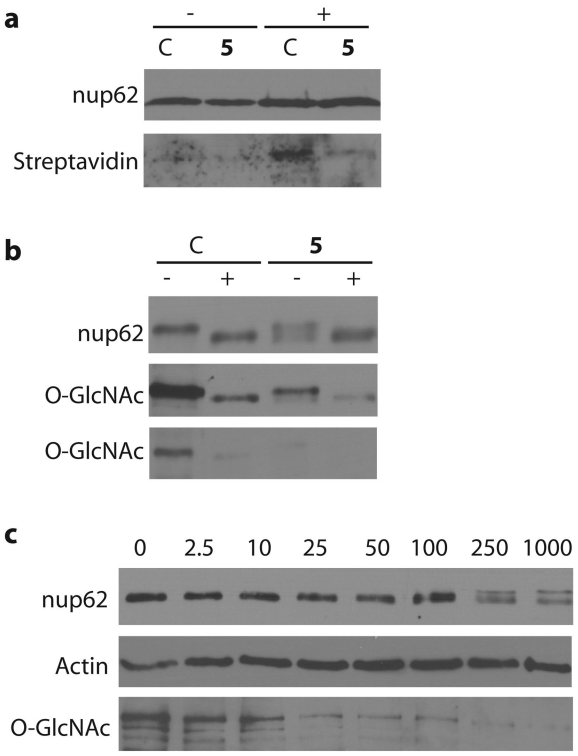

Figure 3. Evaluation of the effects of Ac-5SGlcNAc (5) treatment of cells on the *O*-GlcNAc modification state of nup62

(a) Western blots of immunoprecipitated nup62 from cell lysates following vehicle (C) or 250 μM Ac-5SGlcNAc (**5**) treatment for 24 h. Following immunoprecipitation, nup62 was incubated with UDP-GalNAz in the absence (−) or presence (+) of GalT1 and chemoselectively labelled. Upper panel, probed with anti-nup62 antibody; lower panel, probed with streptavidin. (b) Western blots of immunoprecipitated nup62 from cell lysates following vehicle (C) or 250 μM Ac-5SGlcNAc (**5**) treatment for 24 h. Following immunoprecipitation, nup62 was incubated with buffer (−) or with *Bt*GH84 (+) for 2 h to remove *O*-GlcNAc. Upper panel, probed with anti-nup62 antibody; middle panel, probed with anti-*O*-GlcNAc antibody (CTD110.6) (long exposure); bottom panel probed with anti-*O*-GlcNAc antibody (CTD110.6) (short exposure). (c) Western blots of COS-7 cell lysates following Ac-5SGlcNAc (**5**) administration at different doses (0-1000 μM) for 24 h. Blots are probed with (from top to bottom) anti-nup62 antibody, anti-*O*-GlcNAc antibody (CTD110.6) and anti-actin antibody. Full versions of all of these blots are shown in Supplementary Figure 11.

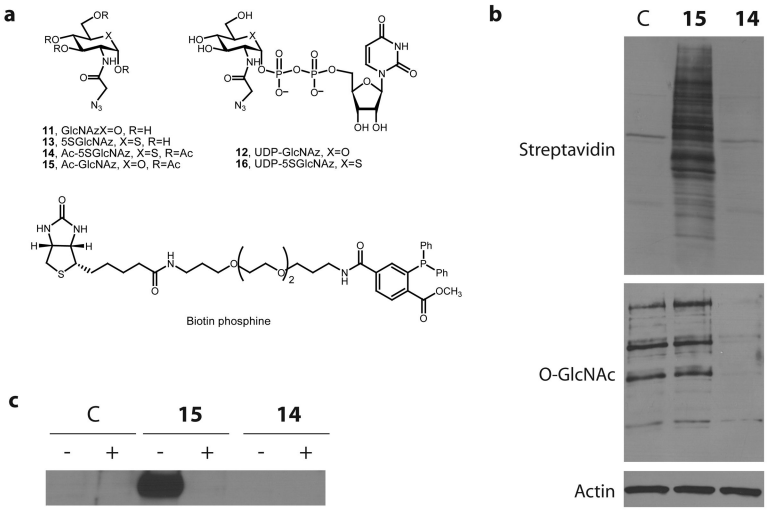

Figure 4. Metabolic feeding of Ac-5SGlcNAz (14) to cells causes a decrease in *O*-GlcNAc levels, but chemoselecctive ligation demonstrates there is no accumulation of 5SGlcNAz (13) on proteins

(a) Structures of the molecules used or generated during the chemoselective ligation study (X = O or S as indicated, R = H or Ac as indicated). (b) Western blots of COS-7 cell lysates administered specified agents at 50 μM for 24 h; vehicle only (C), Ac-GlcNAz (**15**) or Ac-5SGlcNAz (**14**). Cells were harvested and then underwent the Staudinger ligation with biotin phosphine. Blots are probed with (from top to bottom) streptavidin-HRP, anti *O*-GlcNAc (CTD110.6) antibody and anti-actin antibody. (c) Western blot of immunoprecipitated nup62 from cell lysates following vehicle (C), 50 μM Ac-GlcNAz (**15**) or Ac-5SGlcNAz (**14**) treatment for 24 h. Following immunoprecipitation, nup62 was incubated with buffer (−) or with *Bt*GH84 (+) for 2 h to remove *O*-GlcNAc, and then underwent the Staudinger ligation with biotin phosphine. Blots are probed with streptavidin-HRP. A full version of this western blot is shown in Supplementary Figure 13.

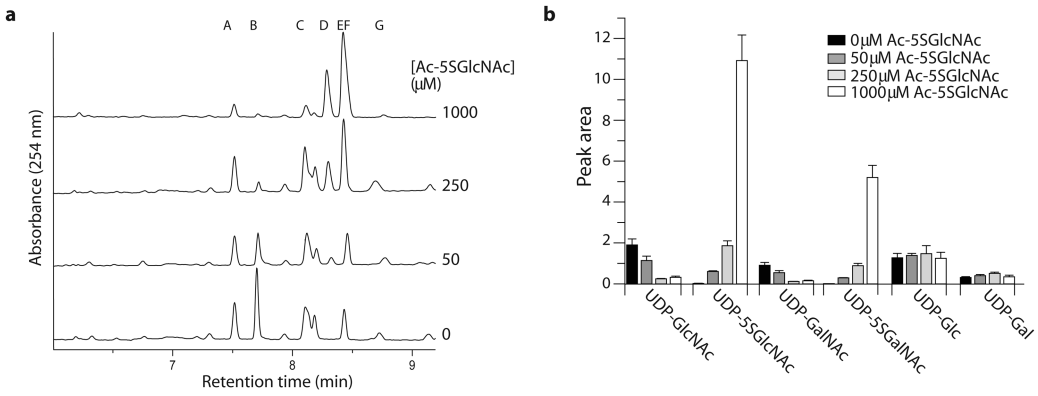

Figure 5. Ac-5SGlcNAc (5) is converted in cells to generate intracellular UDP-5SGlcNAc (4), causing perturbations in UDP-sugar nucleotide pools

(a) Analysis of UDP-sugar pools of COS-7 cells treated with different concentrations of Ac-5SGlcNAc (0-1000 μM from bottom to top) for 24 h; the CE trace shows absorbance at 254 nm as a function of retention time. Peak A, GDP-Glc (internal standard); peak B, UDP-GlcNAc; peak C, UDP-Glc; peak D, UDP-5SGalNAc; peak E, UDP-5SGlcNAc; peak F, UDP-GalNAc; peak G, UDP-Gal. UDP-5SGlcNAc (**4**) and UDP-GalNAc co-elute, but the amount of each is estimated using the epimeric ratios determined from the standards (Supplementary Figure 14b). (b) Bar chart showing relative concentrations of UDP-GlcNAc (**2**), UDP-5SGlcNAc (**4**), UDP-Gal, UDP-5SGal, UDP-Glc, and UDP-Gal following treatment with 0-1000 μM Ac-5SGlcNAc (**5**).

Europe PMC Funders Author Manuscripts

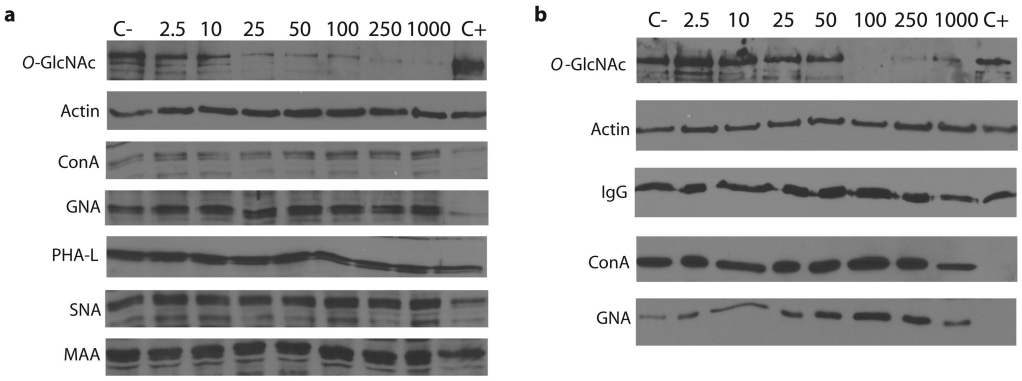

Figure 6. Treatment of cells with Ac-5SGlcNAc (5) has no apparent effects on global *N*-glycosylation or *N*-glycosylation of a secreted IgG as evaluated by lectin blot analysis

(a) Western blots of COS-7 cell lysates following Ac-5SGlcNAc (**5**) administration at different doses (0-1000 μM) for 24 h. C+ denotes untreated cell lysate incubated with PNGase F and C- denotes untreated cell lysate incubated with vehicle. Blots are probed with (from top to bottom) anti-*O*-GlcNAc antibody (CTD110.6), anti-actin antibody, ConA lectin (recognizes α-D-mannose, α-D-glucose and branched mannose), GNA lectin (recognizes mannose), PHA-L (recognizes complex branched chain oligosaccharide structure), SNA lectin (recognizes NeuAcα(2,6)Gal/GalNAc) and MAA lectin (recognizes NeuAcα(2,3)Gal). Full versions of these blots are shown in Supplementary Figure 15a. (b) Western blots of mouse hybridoma cell lysates (*O*-GlcNAc and actin) and immunoprecipitated mouse hybridoma antibody (IgG, ConA and GNA) following administration of Ac-5SGlcNAc (**5**) at different doses (0-1000 μM) for 24 h. C+, untreated cell lysate incubated with PNGase F; C-, untreated cell lysate incubated with vehicle. Blots are probed with (from top to bottom) anti-*O*-GlcNAc antibody (CTD110.6), anti-actin antibody, anti-IgG antibody, ConA lectin and GNA lectin. Full versions of these blots are shown in Supplementary Figure 15b.

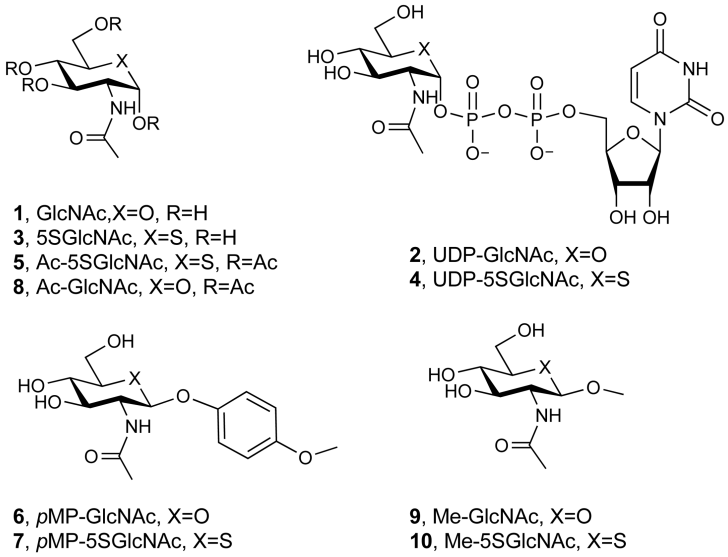

Figure 7.

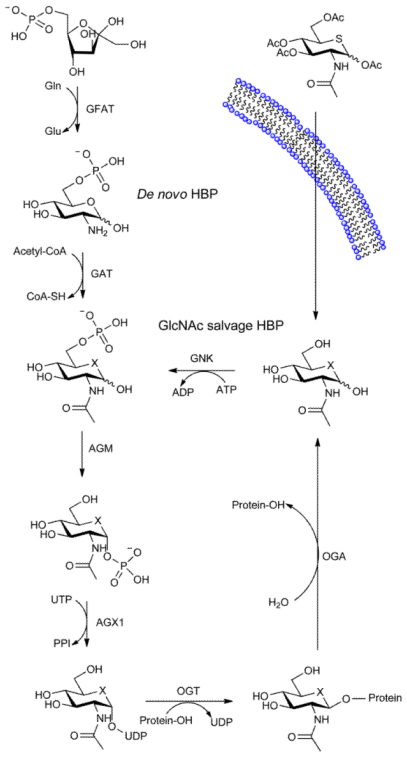

Figure 8.

Europe PMC Funders Author Manuscripts

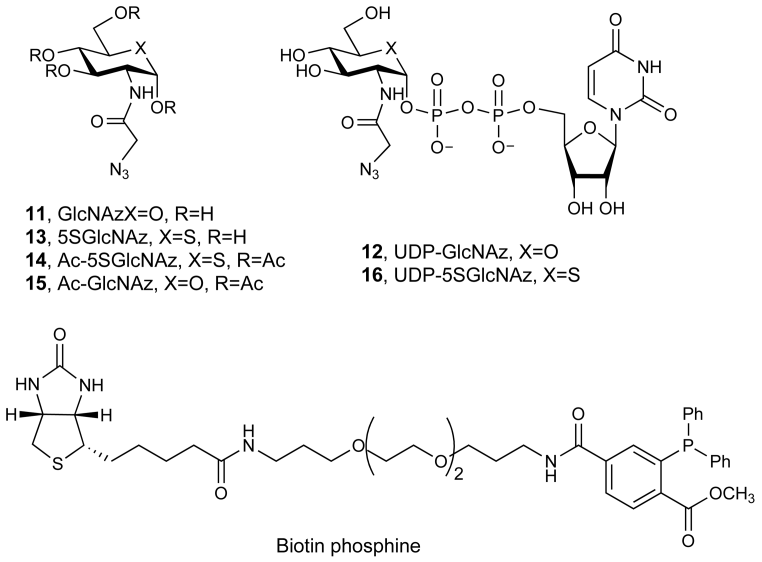

Figure 9.

Europe PMC Funders Author Manuscripts

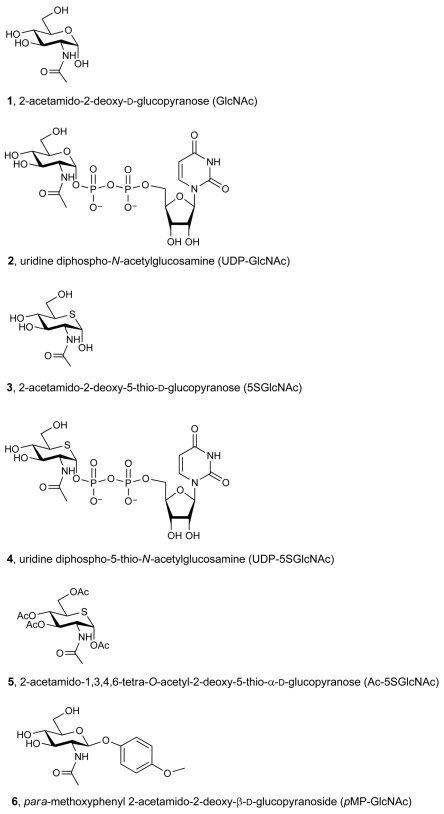

Figure 10.

Europe PMC Funders Author Manuscripts

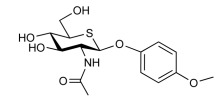

7, *para*-methoxyphenyl 2-acetamido-2-deoxy-5-thio-β-D-glucopyranoside (*p*MP-5SGlcNAc)

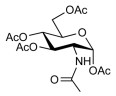

8, 2-acetamido-1,3,4,6-tetra-O-acetyl-2-deoxy-α-D-glucopyranose (Ac-GlcNAc)

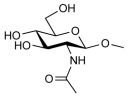

9, methyl 2-acetamido-2-deoxy-β-D-glucopyranoside (Me-GlcNAc)

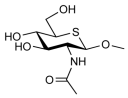

10, methyl 2-acetamido-2-deoxy-5-thio-β-D-glucopyranoside (Me-5SGlcNAc)

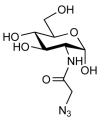

11, 2-azidoacetamido-2-deoxy-D-glucopyranose (GlcNAz)

Figure 11.

Europe PMC Funders Author Manuscripts

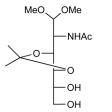

18, 2-acetamido-2-deoxy-3,4-*O*-isopropylidine-aldehydo-D-glucose dimethyl acetal

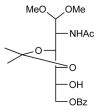

19, 2-acetamido-6-*O*-benzoyl-2-deoxy-3,4-*O*-isopropylidene-aldehydo-D-glucose dimethyl acetal

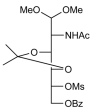

20, 2-acetamido-6-*O*-benzoyl-2-deoxy-3,4-*O*-isopropylidine-5-*O*-mesyl-aldehydo-D-glucose dimethyl acetal

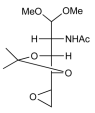

21, 2-acetamido-5,6-anhydro-2-deoxy-3,4-*O*-isopropylidene-aldehydo-L-idose dimethyl acetal

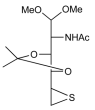

22, 2-acetamido-2,5,6-trideoxy-5,6-epithio-3,4-*O*-isopropylidine-aldehydo-D-glucose dimethyl acetal

Figure 13.

Europe PMC Funders Author Manuscripts

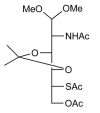

23, 2-acetamido-6-*O*-acetyl-5-*S*-acetyl-2-deoxy-3,4-*O*-isopropylidine-5-thio-aldehydo-D-glucose dimethyl acetal

24, 2-acetamido-3,4,6-tri-*O*-acetyl-2-deoxy-5-thio-α-D-glucopyranose

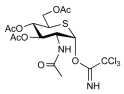

25, 2-acetamido-3,4,6-tri-*O*-acetyl-2-deoxy-5-thio-α-D-glucopyranosyl trichloroacetimidate

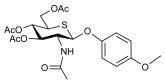

26, *para*-methoxyphenyl 2-acetamido-3,4,6-tri-*O*-acetyl-2-deoxy-5-thio-β-D-glucopyranoside

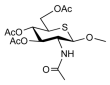

27, methyl 2-acetamido-3,4,6-tri-*O*-acetyl-2-deoxy-5-thio-β-D-glucopyranoside

28, 1,3,4,6-tetra-*O*-acetyl-2-azido-2-deoxy-5-thio-α-D-glucopyranoside

Figure 14.

Europe PMC Funders Author Manuscripts

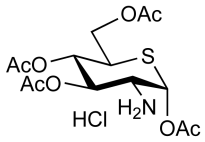

29, 2-amino-1,3,4,6-tetra-*O*-acetyl-5-thio-alpha-α-D-glucopyranose hydrochloride

Figure 15.